Journal of Environmental Sciences Studies

Journal home page: www.jess.ir

Optimization of Hybrid Geothermal–Solar Power Plant Based on Advanced Exergy Analysis Using Genetic and Water Cycle Algorithm

Massome Alibaba [a], Razieh Pourdarbani [a*], Mohammad H. Khoshgoftar Manesh [b], Sina F. Ardabili [a]

[*]a.Biosystem Engineering Dept., University of Mohaghegh Ardabili, Ardabil, Irans
b.Department of Mechanical Engineering, University of Qom, Qom 37161-46611, Iran
Email Address: Razieh Pourdarbani (r_pourdarbani@uma.ac.ir)

Received: (November-21-2021)
Accepted: (January-15-2022)

Abstract

In recent years, human endeavors have been increased to optimally produce clean energy from renewable sources to preserve non-renewable resources and reduce environmental pollution. Economic and environmental analysis based on advanced exergy is a good way to examine the strengths and weaknesses of power generation systems. This paper used advanced exergy analysis to optimize the exergy efficiency of two systems, i.e. standalone geothermal and a hybrid geothermal-solar system. Three-objective optimization was performed by considering twelve decision variables of genetic algorithm and water cycle algorithm. The results of advanced exergy analysis showed that the condenser had the highest avoidable exergy degradation. In the hybrid geothermal-solar cycle, the solar collector became unavoidable in terms of exergy degradation. Exergy degradation of the standalone geothermal cycle was mostly endogenous (78.53%), the maximum avoidable exergy in this cycle was for the ORC evaporator (91.68%). Advanced economic exergy analysis in the hybrid cycle showed that the steam evaporator had the main cost of purchasing equipment in the system. For all components studied, the endogenous cost rate was higher than the exogenous part, indicating a weak relationship between them. The results of genetic algorithms and the water cycle algorithm are very close to each other. In optimization by genetic algorithm, the exergy efficiency of the system has been increased by 1.22%. System costs dropped by 22.49%. The system's environmental impact rate has been dropped from 204.53 mPh to 142.87 mPh. Also, optimization by the water cycle algorithm has increased the exergy efficiency by 1.13% and reduced costs by 21.97%.

Keywords

Energy; Exergy; Renewable energies; Optimization; Genetic algorithm

Introduction

Since the use of solar energy is inherently intermittent, geothermal energy can provide basic power. However, geothermal sources decrease over time by temperature or flow velocity. By combining solar and geothermal power plants, the benefits of both technologies can be used. There are several methods for hybridizing solar and geothermal technologies, and their efficiency depends on factors such as location, the relative quality of geothermal and solar resources (MC Tigio et al., 2018).Exergy, such as enthalpy, is a thermodynamic characteristic that measures the ability of materials to work and includes chemical and physical components. Exergy is mainly used in the early stages of development to achieve better structures, chemical processes, engines, and others. Exergy is defined as the maximum theoretical work that a system can achieve when logging in (Alibaba et al., 2020a).Conventional analysis of exergy examines the system thermodynamically and describes the level of exergy degradation (ED) in each piece of equipment and its thermodynamic causes (James et al, 2015). While advanced analysis evaluates the effects between components of the entire system and measures the real potential for improving one component in the system. In fact, the exergy degradation of each piece of equipment is divided into endogenous and exogenous components as well as avoidable and avoidable components (Alibaba et al., 2020 b).Boyagchi and Heidarnejad (2015) studied a hybrid solar-geothermal cycle. According to the results, thermal efficiency, exergy efficiency, and product cost rates are 23.66%, 9.51%, and 5114.5 $/s, respectively in the summer season. But in the winter, the values were 48.45%, 13.76%, and 5688.1 $/s, respectively. The results of optimization showed that improvement for thermal efficiency, exergy efficiency, and overall cost rate of products were by 28%, 27%, and 17%, respectively in summer while they were by 4%, 13%, and 4% in winter. Rashidi and Khorshidi (2018) investigated the system of simultaneous production of power by exergo-economic analysis. They performed the

optimization on the cycle using the differential evolution (DE) algorithm and the results were verified by (Vazini, 2019). Herberle et al. (2017) technologically and economically analyzed a solar-geothermal power plant of the Rankin cycle. Islam et al. (2017) evaluated an integrated multi-power system based on a hybrid solar-geothermal energy. Ramos et al. (2017) investigated a hybrid solar heat collector with photovoltaic heating systems to generate renewable heat. Anetor et al. (2020) used conventional and advanced analysis to investigate the factors for improving the 750 MW supercritical steam power plant of refined coal. The results showed that the condenser had the most exergy degradation, followed by the boiler.The basic limitations of advanced analysis of exergy can be overcome by optimization. In engineering, many optimizations and decision-making issues are instinctively multi-objective. In most cases, engineers and decision-makers seek to achieve different and sometimes conflicting goals e.g. the subject of quality and cost of production (Yazdanpanah and Barakati, 2016). The main problem in solving multi-objective optimization problems arises from the fact that there is rarely a single point that optimizes all objectives simultaneously and as much as possible. Instead, one should look for a satisfactory balance between these answers and identify a set of optimal answers. Then, according to the decision-maker, one of those points is selected as the optimal point. Evolutionary algorithms have the ability to generate several potential answers to problems, and the choice of the final answer is up to the user. Therefore, they are known to be very efficient in solving problems such as multi-objective optimization (Alavi et al., 2018). Gorbani and Khoshgoftar Manesh (2020) presented a modified hybrid system including solid oxide fuel cell, gas turbine with organic Rankine cycle (ORC), and then thermodynamically modeled and simulated to evaluate its performance. The thermodynamic results of the simulation showed that the net power and overall efficiency of the proposed cycle were increased by 1.1 MW and 7.7%, respectively, compared to the original system.

In the present paper, genetic and water cycle algorithms were used for optimization. Genetic algorithms (GA) are part of evolutionary algorithms in which chromosomes (candidate solution for an optimization problem) result in a more appropriate solution. Using a genetic algorithm, a design is created. Data is then specified for several different variables, for example around 20 variables. Then the genetic algorithm is implemented and examines the best function and variables. The water cycle algorithm (WSA) is used to estimate the parameters of the cycles. This nature-inspired algorithm works based on how streams and rivers flow downhill to the sea and vice versa. In this method, the population matrix, called raindrops, is made up of seas, rivers, and streams. In each repetition, these streams flow into each other and lead to great discoveries in the space of exploration (Alexander and Lange., 2011; Shirin Zaban et al., 2019).In general, in previous research, a system is evaluated only from an economic or environmental point of view. Exergo-conomic and exergo-environmental analyses were evaluated. Optimizations were also performed for both systems by genetic and water cycle algorithms.

2. Materials and Methods

2.1. Explanation of proposed hybrid solar-geothermal power plant

The cycles of the proposed hybrid system include the solar cycle, the upstream steam cycle, middle coupling cycle, the downstream Rankin cycle, and the geothermal cycle coupled by an intermediate system. The heat of saltwater with a temperature of 150°C and a pressure of 1bar is transferred to the downstream working fluid R114 of the ORC and supports the hybrid system at night. The heat transfer fluid (HTF) in the upstream steam cycle receives thermal energy from the lubricant oil flowing at the center of the linear parabolic collector (LPC) solar collectors at 395°C. In the upstream cycle, the temperature of HTF fluid is 395°C when exits the super-heater. Then enters the steam turbine and left there at 170°C. During the day, all the heating power is transferred to the upstream cycle through the solar section and provides the healing power of the hybrid system, and then it transfers and stores some of the heat energy to the geothermal cycle by passing through the middle cycle. At night, when there is no solar thermal energy, the energy stored in the geothermal section is used for heating.

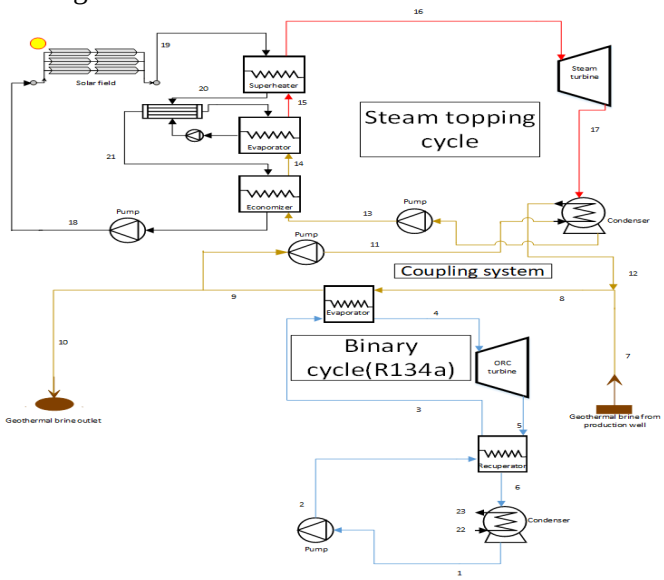

Figure 1. General schematic of a hybrid power plant producing geothermal-solar power

2.2. Simulation of system

Two simulation models have been investigated: the first mode is a standalone geothermal system, when adding a solar part is not economical and the second

mode is a hybrid geothermal-solar based system. Initial model was obtained by Thermo-flow software in which thermodynamic calculations were performed using the refprop9 database, temperature, pressure, and enthalpy of unknown points of the system. Then, the data were analysed by using MATLAB software. The required thermodynamic equations are given in Table (1). Equations (1), (2), and (3) are related to mass, materials, and energy, respectively. The exergy equations are given in Table (2). Equations (4) to (7) are the equations needed to calculate the total exergy rate.

Table 1. Thermodynamic equations required for system modeling (Alibaba et al., 2020)

Definition	Equation
$\sum \dot{m} = 0$	(1)
$\sum \dot{m}x = 0$	(2)
$\sum \dot{Q} + \sum \dot{W} + \sum \dot{m}h = 0$	(3)

Table 2. Exergy equations required to model the system (Yunus et al. 2018, Almutairi et al. 2015)

Definition	Equation
$\dot{E} = \dot{E}^{ph} + \dot{E}^{ch} + \dot{E}^{pe} + \dot{E}^{ke}$	(4)
$\dot{E}^{ph} = \dot{m}[(h_i - h_o) - T_0(s_i - s_o)]$	(5)
$\dot{E}^{ch} = \dot{m}[\sum_{i=1}^{n} x_i e_{0,i}^{ch} + RT_0 \sum_{i=1}^{n} x_i \ln(x_i)]$	(6)
$\dot{E}^{ke} = \frac{1}{2}\dot{m}V^2$	(7)
$\dot{E}^{pe} = \dot{m}gz$	(8)
$\dot{E}_k = \dot{m}_k \cdot e_k$	(9)
$\dot{E}_D = \dot{E}_F - \dot{E}_P = \sum \dot{E}_{in} - \sum \dot{E}_{out} + \sum \dot{Q}\left(1 - \frac{T_0}{T}\right) + \sum \dot{W}$	(10)
$\psi_k = \dot{E}_{P,k} / \dot{E}_{F,k}$	(11)

The total exergy rate includes $\dot{E}^{ph}$ (The physical exergy rate), $\dot{E}^{ch}$ (The chemical exergy rate), $\dot{E}^{pe}$ (The potential, $\dot{E}^{ke}$ (The kinetic), n (The number of moles of the mineral in terms of mol.kg-1), $e_{0,i}^{ch}$ (The standard chemical exergy), x_i (The mole indicator in the inorganic substance of component) and R= 0.0083145 kJ (mol.K)-1 .The reduction of efficiency is not only due to the poor performance of each piece of equipment but also the performance of other equipment has a direct impact on the performance of each piece of equipment. Therefore, advanced exergy analysis considers equipment irreversibility (endogenous and exogenous irreversibility) and the ability to improve irreversibility (inevitable irreversibility) (Akbari and Sheikhi .,2017). To calculate the endogenous irreversibility, first, a hybrid system was designed in which all the equipment works in a theoretical or ideal state, in which the endogenous irreversibility is obtained. Part of the irreversibility that has always existed and is not dependent on the technical and economic constraints of process design is irreversibility. Also, the part of irreversibility that can be eliminated with the least cost and equipment modification is called avoidable irreversibility (Alibaba et al., 2020).

2.3. Optimization Process

After performing advanced exergy analysis and determining the results, the process of optimizing the modifiable equipment is performed in order of priority. As mentioned above, the optimization was performed by genetic and multi-objective water cycle algorithms, then obtained results were compared.Genetic algorithms (GA) are part of evolutionary algorithms in which chromosomes (candidate solution for an optimization problem) result in a more appropriate solution. Using a genetic algorithm, a design is created. Data is then specified for several different variables, for example around 20 variables. Then the genetic algorithm is implemented and examines the best function and variables. The water cycle algorithm (WSA) is used to estimate the parameters of the cycles. This nature-inspired algorithm works based on how streams and rivers flow downhill to the sea and vice versa. In this method, the population matrix, called raindrops, is made up of seas, rivers, and streams. In each repetition, these streams flow into each other and lead to great discoveries in the space of exploration (Alexander et al., 2011; Shirin Zaban et al., 2019).The purpose of the optimization process is to achieve a system that has the maximum systemic efficiency and the lowest cost rate and the lowest environmental impacts. In this paper, three objective functions were investigated in optimization, which is listed in Table (3).

Table 3. Objective functions for cycles

Function	Unit	Symbol
Total exergy efficiency	%	ψ_{Total}
Total Economic exergy rate of system	$\$/h$	$\dot{C}_{Total}$
Total ecological exergy rate of system	mpt/h	$\dot{B}_{Total}$

The execution time for the calculation of the above objective functions was about 0.126s. The optimization improved the answers and reduced the error of objective functions to zero due to the elimination of the production stage of mathematical functions, which is more desirable. Twelve decision variables were selected to do the optimization process (Table 4).To find the best optimal solution, it is better to first rewrite the objective functions in the Pareto optimal solution set to neutralize the effect of the difference in the dimensions of the functions in the sense of the distance of points from the ideal point. Hereupon, the following

equation was used (Sheikhi et al., 2014; Tahmasbzadeh Baei, 2016):

$$OF_{DL,i,k} = \frac{OF_{i,k} - OF_{min,i}}{OF_{max,i} - OF_{min,i}} \quad (1)$$

Table 4. Decision variable and constraint range for variables in optimization process

No	Variable	Constraint	Unit	Symbol
1	Isentropic efficiency of coupling pump	70 – 90	%	η_{CP}
2	Isentropic efficiency of pump in Rankin cycle	70 – 90	%	η_{ORCP}
3	Isentropic efficiency of turbine	70 – 90	%	η_{ORCT}
4	Isentropic efficiency of steam pump	70 – 90	%	η_{SP}
5	Isentropic efficiency of steam turbines	73 – 90	%	η_{ST}
6	Mass flow of geothermal brine	50 – 150	kg/s	m_{brine}
7	Outlet brine temperature	110 – 200	C	$T_{brine,out}$
8	Turbine inlet temperature of Rankin cycle	125 – 200	C	$T_{ORCT,in}$
9	Inlet temperature of Steam turbine	300 – 420	C	$T_{ST,in}$
10	Inlet pressure of Steam turbine	50 – 80	bar	$P_{ST,in}$
11	Outlet temperature of solar collector	300 – 420	C	$T_{SF,out}$
12	Optimal efficiency of solar collector	60 – 80	%	η_{CP}

Where $OF_{DL,i,k}$ is the dimensionless objective function for the i[th] function and the kth response, i is the target function counter and k is the response counter in that target function.In the 3D matrix space, the point is called the coordinate point (1, 0, 0), the equilibrium point, or the ideal point. From the set of optimal answers of Pareto, any answer that is closer to the ideal point is introduced as the selected optimal answer. Equation 2 was used to find the closest answer to the ideal point.

$$d_k = \sqrt{(OF_{1,K} - OF_{1,ideal})^2 + (OF_{2,K} - OF_{2,ideal})^2 + (OF_{3,K} - OF_{3,ideal})^2} \quad (2)$$

3. Results and Discussions

3.1. Conventional analysis of exergy

Thermodynamic information of system for two-mode of geothermal power plant (GPP) and solar-geothermal power plant (SGPP) was obtained by initial simulation in MATLAB (Table 5).The analysis of exergy degradation for the GPP cycle showed that the ORC turbine with 950 kW has the highest exergy degradation rate which accounts for 38% of the total exergy destruction. The maximum investment cost and cost of exergy degradation are related to the ORC turbine. According to the environmental exergy, the OCR turbine has the highest environmental impact rate and the highest environmental impact due to exergy degradation (Table6).Table 7 represents the results of exergy degradation for the SGPP system. It is understood that the solar power plant includes 59% of the total exergy degradation and has the maximum investment cost of the cycle and the lowest cost of exergy degradation. According to environmental exergy, the solar panel had the highest environmental impact rate among the equipment.

Table 5. Thermo-physical properties and exergy values for GPP and SGPP cycle.

State	GPP cycle					SGPP cycle				
	$\dot{m}$ kg.s^{-1}	T (°C)	P (bar)	h (kJ.kg^{-1})	$\dot{E}_x$ (kw)	$\dot{m}$ kg.s^{-1}	T (°C)	P (bar)	h (kJ.kg^{-1})	$\dot{E}_x$ (kw)
1	135.5	35.9	3	235.3	866.4	135.5	35.9	3	235.3	866.4
2	135.5	37.12	21.9	236.9	1049.4	135.5	37.12	21.9	236.9	1049.4
3	135.5	53.76	21.6	253.9	1266.4	135.5	53.76	21.7	253.9	1266.4
4	135.5	130	21.03	410.9	6282.7	135.5	130	21	410.9	6282.7
5	135.5	72.58	3.06	386.4	2476.6	135.5	72.58	3.1	386.4	2476.6
6	135.5	50	3	369.5	2123.9	135.5	50	3	369.5	2123.9
7	100	150	10	632.5	7219	-	-	-	632.5	7219
8	100	150	10	632.5	10355	100	150	10	632.5	10355
9	100	100	10	419.8	4496.9	100	100	10	419.8	4496.9
10	-	-	-	-	-	69.71	100	10	419.8	3134.9
11	-	-	-	-	-	30.3	100.002	10.2	419.9	1362.6

12	-	-	-	-	-	30.3	150	10	632.5	3136.4
13	-	-	-	-	-	3.156	162.87	60.41	691.1	399.4
14	-	-	-	-	-	3.156	270.8	60.21	1189.2	1046.1
15	-	-	-	-	-	3.156	275.8	60.21	2784.4	3437.9
16	-	-	-	-	-	3.156	390	60	3152.4	4039.3
17	-	-	-	-	-	3.156	162	6.5	2724.5	2554.9
18	-	-	-	-	-	23.2	256.1	12.4	890.2	5489
19	-	-	-	-	-	23.2	395	11.3	1222.40	1053.6
20	-	-	-	-	-	23.2	375.9	11.2	1172.5	9750.6
21	-	-	-	-	-	23.2	285.8	11.1	955.8	6440.2
22	434.4	15	1.013	63.08	0	434.4	15	1.013	63.08	0
23	434.4	25	0.996	104.9	307.3	434.4	25	0.993	104.9	307.3

Table 6. Exergy, Exergo –economic and Exergo –environmental results for GPP cycle

Component	Ex_D (kW)	ψ_k(%)	Z (USD.S^{-1})	C_D (USD.S^{-1})	F(%)	Y (pts.S^{-1})	B_D (pts.kJ^{-1})	f_b(%)
ORC Condenser	950.1578	-	7.21E-04	-	-	4.13E-08	-	-
ORC Evaporator	842.2208	85.62	3.11E-04	1.50E-03	17.42	3.56E-06	0.00E+00	100.0
ORC Pump	59.9911	75.31	5.25E-04	3.36E-04	60.97	2.27E-08	2.43E-07	8.6
ORC Recuperator	135.6746	61.53	2.76E-05	4.70E-04	5.554	1.22E-07	1.69E-07	42.1
ORC Turbine	491.5625	87.09	0.005364067	0.0017	75.89	8.68E-06	6.11E-07	93.4

Table 7. Exergy, Exergo –economic and Exergo –environmental results for SGPP cycle

Component	Ex_D (kW)	ψ_k(%)	Z (USD.S^{-1})	C_D (USD.S^{-1})	F(%)	Y (pts.S^{-1})	B_D (pts.kJ^{-1})	f_b(%)
Coupling Pump	8.6E-02	88.42	2.20E-06	1.76E-06	0.00E+00	1.29E-09	2.89E-09	30.9
HTF Pump	2.0E+00	60.52	6.24E-05	4.11E-05	0.00E+00	8.05E-09	6.75E-08	10.7
ORC Condenser	9.5E+02	-	7.21E-04	-	-	4.13E-08	-	-
ORC Evaporator	8.4E+02	85.62	5.14E-04	1.47E-03	1.74E+01	3.56E-06	0	100.0
ORC Pump	6.0E+01	75.31	5.25E-04	3.40E-04	6.10E+01	2.27E-08	2.43E-07	8.6
ORC Recuperator	1.4E+02	61.53	3.02E-05	4.78E-04	5.55E+00	1.22E-07	1.69E-07	42.1
ORC Turbine	4.9E+02	87.08	5.36E-03	1.70E-03	7.59E+01	8.68E-06	6.11E-07	93.4
SolarField(Collector)	6.4E+03	44.21	2.41E-02	0.00E+00	1.00E+02	2.03E-05	0.00E+00	100.0
Steam Economizer	3.1E+02	67.76	3.26E-04	1.48E-03	1.81E+01	2.33E-07	1.25E-06	15.7
Steam Evaporator	9.2E+02	72.25	7.79E-04	4.41E-03	1.50E+01	2.47E-06	3.73E-06	39.8

Steam Pump	2.2E+00	90.08	2.13E-05	4.47E-05	3.23E+01	3.24E-08	7.35E-08	30.6
Steam Super heater	1.8E+02	76.57	2.59E-04	8.84E-04	2.27E+01	1.29E-05	7.48E-07	94.5
Steam Turbine	1.3E+02	91	3.31E-03	2.18E-03	6.03E+01	8.33E-06	3.33E-06	71.4
Topping Condenser	4.0E+02	-	1.29E-03	-	-	2.73E-08	-	-

3.2. Advanced exergy analysis

According to Table 8, in the GPP cycle, the ORC condenser has a higher avoidable exergy degradation rate and so it is the most effective equipment for reducing irreversibility. In Table 8, the ORC condenser has the highest value for avoidable endogenous degradation ($\dot{C}_{D.K}^{EN,AV}$).According to Table 9, the highest endogenous exergy degradation cost of the geothermal-solar cycle (SGPP) is referred to as the vaporizer and then ORC turbines, steam turbines, and steam economizers, respectively which means the rate of destruction cost of these components is reduced. The environmental effects of the exogenous exergy degradation rate of the steam evaporator and steam pump were greater than those of the exogenous exergy degradation rate that indicates the environmental effects of the steam evaporator and steam pump depend on other equipment while the environmental effects of other equipment can be improved by focusing on the equipment itself.

Table 8 Advanced analysis of exergy, exergo –economic and exergo –environmental results for GPP cycle

Component	$\dot{E}_{D.K}^{EN,AV}$ (kW)	$\dot{E}_{D.K}^{EX,AV}$ (kW)	$\dot{C}_{D.K}^{EN,AV}$ (USD.S^{-1})	$\dot{C}_{D.K}^{EX,AV}$ (USD.S^{-1})	$\dot{B}_{D.K}^{EN,AV}$ (pts.S^{-1})	$\dot{B}_{D.K}^{EX,AV}$ (pts.S^{-1})
ORC Condenser	225.18	56.82	-	-	-	-
ORC Evaporator	102.25	21.98	2.56E-04	3.06E-05	-	-
ORC Pump	8.12	0.96	5.20E-05	6.16E-06	2.40E-08	3.55E-09
ORC Recuperator	9.06	2.23	4.07E-05	7.37E-06	1.45E-08	2.72E-09
ORC Turbine	40.65	6.44	1.74E-04	2.07E-05	6.11E-08	8.24E-09

Table 9. Advanced analysis of exergy, exergo –economic and exergo –environmental results for SGPP cycle

Component	$E_{D.K}^{EN,AV}$ (kW)	$E_{D.K}^{EX,AV}$ (kW)	$C_{D.K}^{EN,AV}$ (USD.S^{-1})	$C_{D.K}^{EX,AV}$ (USD.S^{-1})	$B_{D.K}^{EN,AV}$ (pts.S^{-1})	$B_{D.K}^{EX,AV}$ (pts.S^{-1})
Coupling Pump	0.01	0.00	8.31E-08	4.28E+01	2.58E-10	1.63E-10
HTF Pump	0.19	0.02	1.07E-06	9.88E+00	7.81E-09	1.14E-09
ORC Condenser	82.87	14.33	-	-	-	-
ORC Evaporator	64.39	7.03	9.82E-05	7.64E+00	0	0
ORC Pump	6.75	1.81	1.38E-04	2.47E+01	3.96E-08	1.21E-08
ORC Recuperator	22.81	6.60	7.70E-05	2.56E+01	3.59E-08	1.17E-08
ORC Turbine	58.14	8.51	6.30E-04	1.07E+01	1.19E-07	1.91E-08
SolarField(Collector)	1740.53	773.60	0.00E+00	3.58E+01	0.00E+00	0.00E+00
Steam Economizer	72.34	27.63	4.22E-04	2.16E+01	3.74E-07	9.59E-08
Steam Evaporator	182.59	76.07	1.02E-03	2.76E+01	9.57E-07	3.32E-07
Steam Pump	0.19	0.02	5.37E-06	8.77E+00	1.17E-08	9.67E-10
Steam Super heater	31.79	11.02	2.08E-04	2.67E+01	1.73E-07	6.70E-08
Steam Turbine	9.94	0.96	3.43E-04	9.64E+00	5.94E-07	5.71E-08
Topping Condenser	51.01	7.47	-	-	-	-

3.3. Prioritization of equipment in optimization process

According to conventional exergy analysis, it is possible to prioritize equipment for optimization, i.e. equipment with lower efficiency had priority in optimization. (Table 10).

Similarly, according to advanced exergy analysis of equipment, priorities can be set for optimizing any equipment that has more avoidable degradation (Table 11).

Table 10. Prioritization of equipment for optimization according to conventional exergy analysis

Equipment	Exergy	Economic-Exergy	Enviornmental-Exergy
Turbine of Rankin cycle	9	11	9
Recuperator of Rankin cycle	3	1	7
Condenser of Rankin cycle	---	---	---
Evaporator of Rankin cycle	8	5	11
Pump of Rankin cycle	6	10	1
Steam turbine	12	8	8
Steam condenser	---	---	---
Steam pump	11	6	4

Steam economizer	4	3	3
Steam evaporator	5	2	6
Steam Superheater	7	4	10
solar collector	1	12	11
Coupling pump	10	7	5
HTF pump	2	9	2

Table 11. Prioritization of equipment for optimization according to advanced exergy analysis

Equipment	Exergy	Economic-Exergy	Enviornmental-Exgergy
Turbine of Rankin cycle	7	6	6
Recuperator of Rankin cycle	5	5	5
Condenser of Rankin cycle	9	---	---
Evaporator of Rankin cycle	11	10	10
Pump of Rankin cycle	8	8	8
Steam turbine	12	7	7
Steam condenser	6	---	---
Steam pump	10	9	9
Steam economizer	2	1	1
Steam evaporator	3	3	3
Steam Superheater	4	4	4
solar collector	1	2	2
Coupling pump	7	6	6
HTF pump	5	5	5

3.4. Results of three-objective system optimization

After determining the Pareto optimal by genetic algorithm and water cycle algorithm, dimensionless values for objective functions and decision variables were obtained. The isometric and three-dimensional diagrams obtained from the Pareto front as a function of the three objectives obtained by the genetic algorithm and water cycle algorithm are represented in Figures 2 and 3.

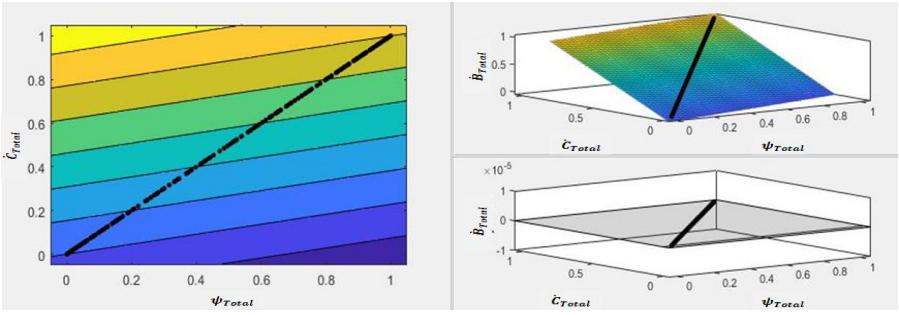

Figure 2. Diagram of dimensionless values of the Pareto optimal functions obtained by GA

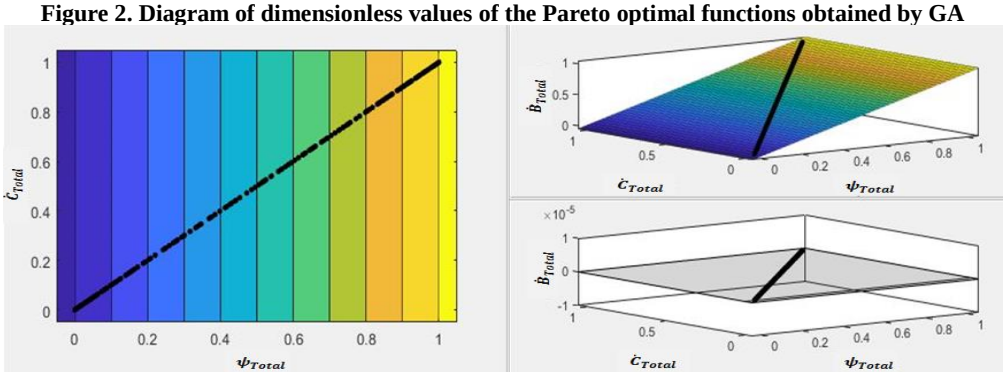

Figure 3. Diagram of dimensionless values of the Pareto optimal functions obtained by WCA

3.5. Optimization results

The selected optimal candidates corresponding to the shortest distance on the Pareto front with the ideal point are listed in Table (15).

Table 15. Selected Optimal Responses for Object Functions Corresponding to the Minimum Distance of Parity Front

	Ψ_{Total} %	$\dot{C}_{Total}$ \$/h	$\dot{B}_{Total}$ mP/h				
Genetic Algorithm	33.16	123.98	142.87				
Water cycle Algorithm	33.07	124.80	145.26				
Values before optimization	31.94	159.96	204.53				

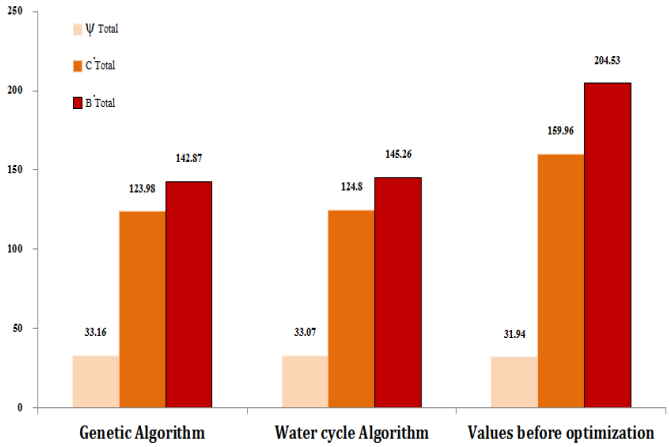

Figure 4. Diagram of Selected Optimal Responses for Object Functions Corresponding

For the optimization by genetic algorithm, the exergy efficiency of the system has increased by 1.22% and reached 33.16%. System costs dropped by 22.49% and reached 123.98 $/h. The rate of the environmental impact of the system decreased by 30.15% and reached 142.87 mP/h (mili point/hour).Also, for optimization by the water cycle algorithm, the exergy efficiency of the system has increased by 1.13% and reached 33.07%. System costs dropped by 21.97% and reached 124.80 $/h. The system's environmental impact rate has dropped by 28.97% and reaches 145.26 mP/h.Comparison of results in Figure (4), the objective functions of genetic and the water cycle algorithms were compared. It can be found that the results of the two algorithms are almost similar.

3.6. Optimal responses of decision variables on the Pareto front with the ideal point

Table (16) gives the optimal responses for decision variables. The optimal isentropic efficiency of coupling pump, ORC pump, steam pump, and steam turbine in the genetic algorithm have been increased by 5, 10, 5, and 0.9% while the optimal isentropic efficiency of ORC turbine and solar collector has been reduced by 6.9 and 14.1%. It is intended to reach the optimum point in terms of exergy efficiency, cost rate, and environmental impact rate, coupling pump, ORC pump, and steam pump must operate with higher isentropic efficiency but the turbine and solar collector must operate with lower isentropic efficiency.

Table 16. Selected optimal answers for decision variables corresponding to the shortest distance on the Pareto front with the ideal point

	η_{CP}	η_{ORCP}	η_{ORCT}	η_{SP}	η_{ST}	m_{brine}	$T_{brine,out}$	$T_{ORCT,in}$	$T_{ST,in}$	$P_{ST,in}$	$T_{SC,out}$	$\eta_{coll,opt}$
	[-]	[-]	[-]	[-]	[-]	[kg/s]	[C]	[C]	[C]	[bar]	[C]	[-]
GA	0.900	0.900	0.781	0.900	0.879	52.168	147.620	192.595	350.000	65.000	420.000	0.600
WCA	0.738	0.856	0.831	0.795	0.881	50.338	183.436	168.398	407.620	64.555	383.872	0.757
Values before optimization	0.850	0.800	0.850	0.850	0.870	100.000	150.000	130.000	390.000	60.000	395.000	0.741

It can also be seen in Figure (5) that the optimal isentropic efficiency of ORC pump, steam turbine, and solar collector in water cycle algorithm is considered to be 10, 1.1, and 1.6%, respectively, while these values for coupling pump, ORC turbine, and steam pump decreased by 11.2, 5.6 and 5.5%. According to the results of the water cycle algorithm, although ORC pump and steam turbine work with higher isentropic efficiency after optimization, coupling pump, turbine, and steam pump should work with lower isentropic efficiency so that the system can reach its optimum point in terms of exergy efficiency, cost rates, and environmental impact rates.

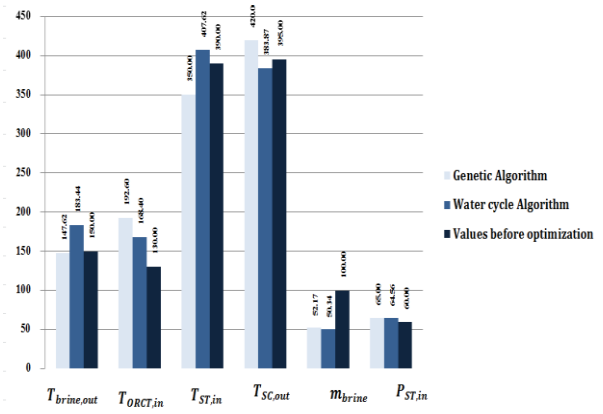

Figure 6. Selected optimal answers for other decision variables

According to table (16), the optimum mass flow rate of geothermal brine in the genetic algorithm and water cycle algorithm was considered to be about half of the value before optimization, and this helps maintain geothermal water reserves. The optimum temperature of the outlet brine is reduced by about 3°C in the genetic algorithm, and even less depth can be considered for the geothermal part. However, in the optimization by the water cycle algorithm, 33°C was added to the optimal temperature of the outlet brine, and the geothermal part should be deeper, or this amount of temperature increase should be compensated by the auxiliary temperature of the solar collector part.Figure (6) shows that the optimal values of decision variables, the optimal temperature of the fluid enteringthe turbine and steam pump in the genetic algorithm increased by 60 and 25°C, respectively, and the optimal temperature of the fluid entering the steam turbine decreased by 40°C. Also, the optimal pressure of the inlet fluid to the steam turbine increased 5 times. The optimum temperature of the inlet fluid to the ORC turbine and the steam turbine in the water cycle algorithm increased by 38 and 17°C, respectively. The optimum temperature of the inlet fluid to the steam pump decreased by 12°C. Also, the optimal pressure of the inlet fluid to the steam turbine

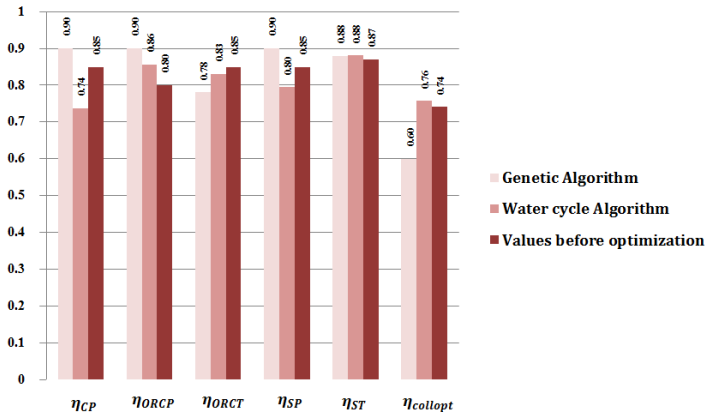

Figure 5. Selected optimal responses for equipment efficiency as a decision variable

is increased 4.5 times so that the system reaches its optimal point in terms of exergy efficiency, cost rate, and environmental impact rate.

4. Discussion and conclusion

- In the present paper, conventional and advanced exergy-based analyses were performed for a hybrid solar-geothermal power plant. Thus, the problem of incompatibility of the outlet temperature of the solar collectors of the power plant (about 395°C) with the desired temperature of the binary geothermal part (about 150°C) is solved and this is one of the advantages of this research over other researchers in designing hybrid power plants. Because solving this problem with other methods requires changing the equipment and sometimes this may be impossible. In the present study, in a hybrid power plant, using the upstream solar cycle and adding the Rankin cycle, without the need for any additional equipment, the advantage of additional heating power generated in summer and conservation of internal heat sources can be exploited.Conventional and advanced exergy analysis of hybrid geothermal-solar and standalone geothermal cycles was performed. Comparisons between conventional and advanced analysis resulted in a similar effect on each component, but the advanced exergy approach showed a slightly higher value, meaning that advanced exergy analysis is more accurate.Finally, the optimization of the desired cycle was done using genetic algorithms and a multi-objective water cycle algorithm.

References

- Akbari, N.; Sheikhi, S. Optimization and advanced exergy evaluation of a Clausius-Rankine cycle to be used in solar power systems. Modares Mech. Eng. **2017**, 17, 333–342.
- Alavi, S.R.N., K.Ateshkari., M.A. Alipour., R.K. Kamali, 2018. Exergy-economic simulation and

optimization of a triple production system. Energy Engineering and Management, 8 (1), 40-53.
- Alexander, D.H., Lange, K. Enhancements to the ADMIXTURE algorithm for individual ancestry estimation. BMC Bioinformatics **12,** 246 (2011). https://doi.org/10.1186/1471-2105-12-246.
- Alibaba, M.; Pourdarbani, R.; Manesh, M.H.K.; Miranda,I.H.; Bernal.I.H.; Hernández,J.L.H.Conventional and Advanced Exergy-Based Analysis of Hybrid Geothermal–Solar Power Plant Based on ORC Cycle.MDPI,Applied Sciences,2020, 10, 5206 ; doi:10.3390/app10155206.
- Alibaba, M.; Pourdarbani, R.; Manesh, M.H.K.; Ochoa, G.V.; Forero, J.D. Thermodynamic, exergo-economic and exergo-environmental analysis of hybrid geothermal-solar power plant based on ORC cycle using emergy concept. Heliyon 2020, 6, e03758.
- Almutairi, S.A., P. Pilidis, N. Al-Mutawa, 2015. Energetic and Exergetic Analysis of Combined Cycle Power Plant: Part-1 Operation and Performance. Energies, 8, 14118–14135.
- Anetor, L.; Osakue, E.E.; Odetunde, C. Classical and advanced exergy-based analysis of a 750 MW steam power plant. Aust. J. Mech. Eng. **2020**, 1–21, doi:10.1080/14484846.2020.1716509.
- Boyaghchi, F.A, P. Heidarnejad, 2015. Thermoeconomic assessment and multi objective optimization of a solar micro CCHP based on Organic Rankine Cycle for domestic application. Energy Conversion and Management, 97: p. 224-234.
- Ghorbani, S., M.H. Khoshgoftar Manesh, 2020.Conventional and Advanced Exergetic and Exergoeconomic Analysis of an IRSOFC-GT-ORC Hybrid System. Gas Process, 8, 1–16.
- Heberle, F.; Hofer, M.; Ürlings, N.; Schröder, H.; Anderlohr, T.; Brüggemann, D. Techno-economic analysis of a solar thermal retrofit for an air-cooled geothermal Organic Rankine Cycle power plant. Renew. Energy 2017, 113, 494–502.
- Islam, S.; Dincer, I. Development, analysis and performance assessment of a combined solar and geothermal energy-based integrated system for multigeneration. Sol. Energy 2017, 147, 328–343.
- James, C., T.Y.Kim, R. Jane, 2020 .A Review of Exergy Based Optimization and Control. Processes, 8, 364.
- McTigue, D.; Castro, J.; Mungas, J.; Kramer, N.; King, J.; Turchi, G.; Zhua, G. Hybridizing a geothermal power plant with concentrating solar power and thermal storage to increase power generation and dispatchability. Appl. Energy **2018**, 228, 1837–1852.
- Ramos Cabal, A.; Guarracino, I.; Mellor, A.; Alonso-Alvarez, D.; Ekins-Daukes, N.; Markides, C. Solar-thermal and hybrid photovoltaic-thermal systems for renewable heating. In Imperial College London; Grantham Institute: London, UK, 2017, pp. 12–14.
- Rashidi, H., and J. Khorshidi, 2018. Exergoeconomic analysis and optimization of a solar based multigeneration system using multiobjective differential evolution algorithm. Journal of Cleaner Production, **170**: p. 978-990.
- Sheikhi,S., B. Ghorbani, R. Shirmohammadi, M.H. Hamedi,2014. Thermodynamic and Economic Optimization of a Refrigeration Cycle for Separation Units in the Petrochemical Plants Using Pinch Technology and Exergy Syntheses Analysis. GasProcessingJournal, 2(2), 2322-3251.
- Shirinzaban, A., H. Barati, M. Nasir, 2019. Optimal Multi-Objective Placement of UPFC for Power Systems Operation Planning Using Water Cycle Optimization Algorithm in Nature, New Scientific-Specialized Journal of Electricity, 8 (1), 47-59
- Tahmasbzadeh, M. ،H. Sayadi, 2016. Optimization of gas turbine cycle with right-fin plate heat exchanger to increase performance and reduce pollutants. Iranian Journal of Energy, 18 (4), 141-161.
- Vazini, H., 2019. Optimal design of exergetic, economic exergy and environmental exorcist system of simultaneous power generation, fresh water and cooling system based on 25 MW gas turbine and MED-TVC method in Qeshm Island, Master Thesis, Qom University, Faculty of Engineering.
- Yazdanpanah, M. A., S. M. Barakati, 2016. A New Perspective on the Design and Optimization of Renewable Electricity Generation Systems: Evaluating the Conformity Criteria of Power Generation and Consumption with Assessing System Reliability. Journal of Iranian Association of Electrical and Electronics Engineers, 13 (3), 1-12.
- Yunus, E., Y.E. Yuksel, M. Ozturk, 2018. Thermodynamic assessment of an integrated solar collector system for multigeneration purposes. In Exergetic Energetic and Environmental Dimensions, pp. 363–372. Afyon Kocatepe University: Afyon, Turkey.

Appendix A

Table A1. Calculations for Cost rate and environmental destruction rate in the two operating cycle modes. (Alibaba et al., 2020).

component	Cost rate ($\dot{Z}_k$)		environmental destruction rate ($\dot{Y}_k$)	
	Standalone Geothermal	Solar & Geothermal	Standalone Geothermal	Solar & Geothermal
Solar collector	-	0.024	-	2.03e-05
Coupling Pump	-	2.19e-06	-	1.29e-09
HTF Pump	-	6.24e-05	-	8.05e-09
ORC Condenser	7.2e-04	7.2e-04	4.13e-08	4.13e-08
ORC Evaporator	3.11e-04	5.14e-04	3.56e-06	3.56e-06
ORC Pump	5.25e-04	5.25e-04	2.27e-08	2.27e-08
ORC Recuperator	2.75e-05	3.02e-05	1.22e-07	1.22e-07
ORC Turbine	0.0054	0.0054	8.67e-06	8.67e-06
Steam Economizer	-	3.26e-04	-	2.33e-07
Steam Pump	-	2.13e-05	-	3.23e-08
Steam Super heater	-	2.59e-04	-	1.29e-05
Steam Turbine	-	0.0033	-	8.33e-06
Topping Condenser	-	0.0013	-	2.73e-08
Steam Evaporator	-	7.79e-04	-	2.47e-06

Table A2. Correlation of cost and weight function for components. (Alibaba et al., 2020).

component	Weight function: for Eq.(19), Y = b_m. Weight	Cost function: USD,for Eqs.(10) and (11)
Solar collector	ton,m, $w_{Coll} = 0.0626.L$, b_m = 23.2 Cavalcanti [48]	(USD*m^-2), $PEC_{coll} = 355 A_{coll}$ Cavalcanti [48]
Coupling Pump	ton,KW, $w_{CP} = 0.0061(Q_{CP})^{0.95}$, b_m = 132.8 Cavalcanti [48]	$PEC_{CP} = 16800 (W_{CP}/200)^{0.67}$ Bonyadi et al.[26]
HTF Pump	ton,KW, $w_{HTFP} = 0.0061 (Q_{HTFP})^{0.95}$, b_m = 132.8 Cavalcanti [48]	$PEC_{HTPP} = 3540 (W_{HTPP})^{0.71}$ Baghernejad et al.[61]
ORC Condenser	ton,MW,$w_{ORCCon} = 0.073 (Q_{ORCCon})^{0.99}$, b_m = 2.8 Cavalcanti [48]	$PEC_{ORCCon} = 1773 m_{orc\,cycle}$ Nami et al.[62]
ORC Evaporator	ton, MW, $w_{ORCEv} = 13.91(Q_{ORCEv})^{0.68}$, b_m = 28 Cavalcanti [48]	$PEC_{ORCev} = 34.9 A_{ORCev}$ Mehrpooya et al.[58]
ORC Pump	ton,KW, $w_{ORCp} = 0.0631 ln(W_{ORCp})$ -0.197, b_m = 132.8 Cavalcanti [48]	$PEC_{ORCP} = 3540 (W_{ORCP})^{0.71}$ Baghernejad et al.[61]
ORC Recuperator	ton,KW, $w_{ORC\,Rec} = 2.14(Q_{ORC\,Rec})^{0.7}$, b_m = 28 Cavalcanti [48]	$PEC_{ORCrec} = \left(\frac{A_{ORCrec}}{0.093}\right)^{0.78}$ Mehrpooya et al.[58]
ORC Turbine	ton,MW, $w_{ORCT} = 4.90(W_{ORCT})^{0.73}$, b_m = 646 Cavalcanti [48]	$PEC_{ORCT} = \frac{479.34 m_{orc\,cycle}}{0.92 - \eta_{ORCT}}\left(\frac{P_4}{P_5}\right)(1 + e^{(0.036T_{24} - 54.4)})$ Nami et al.[62]
Steam Economizer	ton,MW,$w_{SEco} = 2.430(Q_{SEco})^{1.15}$, b_m = 28 Cavalcanti [48]	$PEC_{SEco} = 235(Q_{SEco})^{0.75}$ Bonyadi et al.[26]
Steam Pump	ton,KW, $w_{Sp} = 0.0061(Q_{Sp})^{0.95}$, b_m = 132.8 Cavalcanti [48]	$PEC_{SP} = 16800 (W_{SP}/200)^{0.67}$ Bonyadi et al.[26]
Steam Super heater	ton,MW,$w_{SSH} = 8.424 (Q_{SSH})^{0.87}$, b_m = 638 Cavalcanti [48]	$PEC_{SSH} = 235 (Q_{SSH})^{0.75}$ Bonyadi et al.[26]
Steam Turbine	ton,MW, $w_{ST} = 4.90(W_{ST})^{0.73}$, b_m = 646 Cavalcanti [48]	$PEC_{sT} = 31093 (W_{sT})^{0.41}$ Bonyadi et al.[26]
Topping Condenser	ton,MW,$w_{Tcond} = 0.073(Q_{Tcon})^{0.99}$, b_m = 28 Cavalcanti [48]	$PEC_{Scond} = 597(W_{Scond})^{0.68}$ Bonyadi et al.[26]
Steam Evaporator	ton, MW, $w_{SEv} = 13.91(Q_{SEv})^{0.68}$, b_m = 28 Cavalcanti [48]	$PEC_{SEV} = 235(Q_{SEV})^{0.75}$ Bonyadi et al.[26]
Variable	w (component Weight), W (work, W) , Q(heat transfer, W) b_m (the environmental impact per weight unit for each component, mpts*kg^-1) A (Area, m^2), L = length,	$\dot{m}$ (mass flow rate (kg*s^-1)), η (efficiency) life of power plant(hours in a year):N_{ORC} = 8100 Number of lifetime (year): n = 30 Interest rate: i = 7.24/100, maintenance factor: Φ = 1.06

Table A3. Equations and theoretical analysis for Component of cycle. (Alibaba et al., 2020).

Component	Relations	Inputs	Outputs
Solar collector	$[Q_u = R_r * Q_{coll} - Q_{loss,abs} - Q_{loss,pipe}]$, $[Q_u = m_{HTF}*(h_{19} - h_{18})$ $[Q_{coll} = eta_{opt}*f_{dust}*M_s*A_{coll}*DNI]$, $[h_{19} = h_{@T:T_{19},P:P_{19}}]$	$h_{18} = 890$, $R_r = 1$, $eta_{opt} = 0.741$, $f_{dust} = 0.98$, $M_s = 1.25$, $A_{coll} = 12225$, DNI =1000, $m_{HTF} = 3.16$	Q_{coll}, $Q_{loss,abs}$ $Q_{loss,pipe}$, Q_u, h_{19}
Coupling Pump	$[W_{Coupling\ Pump} = m_{11}(h_{11} - h_9)]$, $[P_{11} = P_{12}/(1-dp_{Steam\ Condenser})]$ $[h_{11} = (h_{11s} - h_9)/eta_{cp} + h_9]$	$P_{12} = 10$, $dp_{SCond} = 0.2$ $eta_{cp} = 0.85$, $h_9 = 419.8$, m_{11}	W_{cp}, h_{11}, P_{11}
HTF Pump	$[W_{HTF\ Pump} = m_{HTF}(h_{18} - h_{24})]$, $[P_{18} = P_{19}/(1-dp_{Solar\ Field})]$, $[h_{18} = (h_{18s} - h_{24})/eta_{HTFP} + h_{24}]$	$P_{19} = 11.3$, $dp_{Solar\ Field} = 0.1$, $eta_{HTFP} = h_{24} = 419$, m_{HTF}=3.16	W_{HTFP}, h_{18}, P_{18}
ORC Condenser	$[m_{ORC}(h_6 - h_1) = m_{Cool\ WATER}(h_{23} - h_{22})]$,$[T_{23} = T_{22} + deltaT_{Cool\ WATER}]$ $[P_{23} = P_{22}(1-deltaP_{Cooling\ WATER})]$,$[h_1 = h_{@x:0,P:P_{ORCCondenser}}]$, $[h_{22} = h_{@T:T_{22},P:P_{22}}]$,$[h_{23} = h_{@T:T_{23},P:P_{23}}]$	$m_{ORC} = 135$, $h_6 = 369.4$, $h_{22} = 63.07$, $h_1 = 235.3$, $T_{22} = 15$, $P_{22} = 1.01$,$deltaT_{CW} = 10$, $deltaP_{CW} = 0.02$, $P_{ORCCond}$=3	h_1, m_{CW} h_{23}, T_{23}, P_{23}
ORC Evaporator	$[m_{ORC}(h_6 - h_5) = m_{Brine}(h_9 - h_8)]$, $[m_{Brine} = 100(kg/s)]$, $[h_6 = h_{@T:T_6,P:P_6}]$, $[h_5 = h_{@T:T_5,P:P_5}]$, $[h_9 = h_{@T:T_9,P:P_9}]$	$h_5 = 253.9$, $h_8 = 410.8$,$m_{Brine} = 100$	$m_{ORC\ cycle}$, h_5,h_9
ORC Pump	$[W_{ORC\ Pump} = m_{ORC}(h_2 - h_1)]$, $[P_2 = P_2/(1-dp_{ORC\ Recuperator})]$, $[h_2 = (h_{2s} - h_1)/eta_{ORC\ Pump} + h_1]$	$P_2 = 21.7$, $eta_{ORCP} = 0.8$, h_1=235.3	$W_{ORC\ Pump}$, h_2,P_2
ORC Recuperator	$[h_3 - h_2 = h_5 - h_6]$, $[P_6 = P_{ORCCond}]$, $[P_3 = P_3/(1-dp_{ORCEva})]$	$h_2 = 236.9$, $h_5 = 369.5$, $h_3 = 386.3$, $P_{ORCCon} = 3$, $dp_{ORCEva} = 0.03$, $P_2 = 21.9$	h_3, P_6, P_3
ORC Turbine	$[W_{ORCT} = m_{ORC}(h_6 - h_5)]$, $[P_5 = P_6/(1-dp_{ORCRec})]$, $[h_5 = h_6-(h_6 - h_{5s}) * eta_{ORCT}]$, $[P_6 = P_{ORCCond}]$	$m_{ORC} = 135.5$, $h_6 = 410.8$, $P_{ORCCon} = 0.1$ $dp_{ORCRec} = 0.01$, $eta_{ORCT} = 0.85$	$W_{ORC\ Turbine}$, h_5, P_5
Steam Economizer	$[m_{SC}(h_{16} - h_{12}) = m_{HTF}(h_{21} - h_{24})]$, $[h_{16} = h_{@x:0,P:P_{16}}]$	m_{SC}, $h_{12} = 691.07$, $m_{HTF} = 3.16$, $h_{21} = 955.8$	h_{16}, h_{24}
Steam Pump	$[W_{Steam\ Pump} = m_{SC}(h_{12} - h_{25})]$, $[P_{12} = P_{16}/(1-dp_{Economizer})]$, $[h_{12} = (h_{12s} - h_{25})/eta_{SP} + h_{25}]$	$P_{16} = 60.2$, $dp_{ECO} = 0.2$, $eta_{SP} = 0.85$, $h_{25} = 684.08$, m_{SC}	W_{SP}, h_{12}, P_{12}
Steam Super heater	$[m_{SC}(h_{16} - h_{15}) = m_{HTF}(h_{19} - h_{20})]$, $[h_{16} = h_{@T:T_{16},P:P_{16}}]$	m_{SC}, $h_{15} = 2784.4$, $m_{HTF} = 3.16$, $h_{19} = 1222.4$	h_{16}, h_{20}
Steam Turbine	$[W_{Steam\ T} = m_{SC}(h_{16} - h_{17})]$, $[h_{17} = h_{16}-(h_{16} - h_{17s}) * eta_{Steam\ T}]$, $[P_{17} = P_{Steam\ Condenser}]$	m_{SC}, $h_{16} = 3152.4$, $eta_{ST} = 0.87$, $P_{SCond} = 6.5$	$W_{Steam\ T}$, h_{17}, P_{17}
Steam Condenser	$[m_{ST\ Cond}(h_{17} - h_{25}) = m_{11}(h_{12} - h_{11})]$, $[T_{12} = 150\ (C)]$, $[P_{12}$=10(bar)$]$ $[h_{25} = h_{@x:0,P:P_{Steamcondenser}}]$, $[h_{12} = h_{@T:T_{12},P:P_{12}}]$	m_{SC},$h_{17} = 2724.5$,$h_{11} = 419.86$,$T_{12} = 150$, $P_{12} = 10$, $P_{SCond} = 6.5$	h_{25}, h_{12}, m_{11}
Steam Evaporator	$[m_{ST\ Eva}(h_{15} - h_{14}) = m_{HTF}(h_{20} - h_{21})]$, $[h_{15} = h_{@x:1,P:P_{15}}]$, $[h_{21} = h_{15} + \Delta T_{Pinch}]$	$h_{14} = 1189.2$, $m_{HTF} = 3.16$, $h_{20} = 1172.4$	h_{15}, h_{21}, m_{SC}